Physics Procedia

Volume 75, 2015, Pages 1450–1457

20th International Conference on Magnetism

Magnetically modified TiO_2 powders – microstructure and magnetic properties

Ondřej Životský[1,2*], Jana Seidlerová[2], Ivo Šafařík[3], Jiří Luňáček[4], Miroslava Šafaříková[3], Kateřina Mamulová Kutláková[2], Yvonna Jirásková[5]

[1]*Boris Yeltzin Ural Federal University, Ekaterinburg, Russia*
[2]*Nanotechnology Centre, VŠB-Technical University of Ostrava, Ostrava-Poruba, Czech Republic*
[3]*Institute of Nanobiology and Structural Biology of GCRC AS CR, České Budějovice, Czech Republic*
[4]*Institute of Physics, VŠB-Technical University of Ostrava, Ostrava-Poruba, Czech Republic*
[5]*Institute of Physics of Materials, Academy of Sciences of the Czech Republic, Brno, Czech Republic*
ondrej.zivotsky@post.cz, jana.seidlerova@vsb.cz

Abstract

The anatase (TiO_2) particles magnetically modified by iron oxides and prepared by an innovating technological procedure are studied from the viewpoint of microstructure and a complex analysis of magnetic behaviour at room and elevated temperatures. Scanning electron microscopy observations have yielded variable shapes of particles in the composite powder whereas the iron oxide particles of diameter bellow 1 μm were detected on the surface of the TiO_2. The dominant magnetite (Fe_3O_4) accompanied by a small amount of maghemite (γ-Fe_2O_3) and/or hematite (α- Fe_2O_3) were analysed by X-ray powder diffraction. A relatively high saturation magnetization (3.38 Am^2/kg), negative dipolar interactions, and the low values of reversible and irreversible part of magnetic susceptibility were found out from magnetic measurements at room temperature. During a thermomagnetic treatment the composite sample has been going through a few magnetic phase transitions and transforms into a fully paramagnetic state around 850 K. After its cooling to the room temperature an undesirable magnetic hardening of the sample has occurred.

Keywords: Magnetically modified TiO_2, X-ray powder diffraction, microstructure, magnetic properties, vibrating sample magnetometer

* Corresponding authors: Ondrej Zivotsky, phone: +420 597323361

 Selection and peer-review under responsibility of the Scientific Programme Committee of ICM 2015

doi:10.1016/j.phpro.2015.12.165

1 Introduction

Titanium dioxide, occurring in three modifications as anatase, brookite, and rutile, can be used in various technological applications (especially the anatase) such as photovoltaic solar cells, sensors and photocatalytic processes. The TiO_2 photocatalysis is a promising technique for decontamination, purification, and deodorization of air and wastewater [Ollis (1985), Yu et al. (2001)]. It has also been applied to the inactivate bacteria, viruses, and cancer cells [Fu et al. (2005), Hu and Apbelett (2014), Sunada et al. (2003)]. The anatase (TiO_2) particles are a suitable and effective adsorbent for elimination of toxic ions and compounds from aqueous solutions due to their high stability supported by the low cost and safety toward both humans and environment [Konstantinou and Pashalidis (2008), Svecova et al. (2011), Tan et al. (2007), Tsydenov et al. (2014)]. To improve the separation of solid materials including sorbents from liquids the composites with magnetic compounds were designed for such applications. In addition, the magnetic particles are often effective sorbent materials owing to their unique magnetic properties and a good adsorption capacity. The antibacterial activity of TiO_2-based nanostructured Fe^{3+}-doped coatings on glass substrates against *E. coli* has been studied by applying the so-called antibacterial-drop test [Trapalis et al. (2003)]. Sorption properties of Pb^{2+} ions on the magnetically modified anatase were verified and the sorption processes were modeled using the Langmuir and Freundlich isotherms [Seidlerova et al. (2015)]. The results have shown that the particles of the magnetically modified anatase are a suitable material for removing the Pb^{2+} ions from the aqueous solution. Because these systems are not used at high temperature atmospheres, we do not expect marked oxidation of Fe_3O_4 and Fe_2O_3 particles. In addition to the biodegradable and photocatalytic properties of TiO_2 particles, their magnetic modification can be subsequently magnetically purified whereby an efficiency of the wastewater treatment can be enhanced.

The present paper is devoted to the preparation of a magnetically modified anatase (TiO_2) powder and to a detailed analysis of its microstructural and magnetic properties. The main attention is devoted to the room temperature magnetic characteristics, interparticle magnetic interactions, and the behaviour of reversible and irreversible magnetic susceptibility. The composite behaviour and its stability at elevated temperatures are followed by the thermomagnetic measurement.

2 Materials and methods

$TiOSO_4$ (PRECHEZA, a.s.) containing TiO_2 (~102 g/dm^3) was used as a precursor for preparation of the TiO_2 powder. The whole procedure in more details can be found in a previous work [Mamulova Kutlakova et al. (2010)]. The magnetic modification was subsequently done by addition of the TiO_2 powder into $FeSO_4 . 7H_2O$ dissolved in water and slowly mixed under dropping of sodium hydroxide solution until a certain value of pH was reached. During this process it comes to a precipitation of iron(II) hydroxide. The obtained suspension was then diluted by water and inserted into a standard kitchen microwave oven for a certain time. Next, the formed material was repeatedly washed with water and magnetically responsive composite was captured using a magnetic separator. The details can be found in a previous paper [Safarik et al. (2013)]. The important parameters: the total content of Fe, Fe^{II} (expressed as content of FeO), the specific surface area (ssa), and the mean diameter of the non-magnetically and the magnetically modified anatase particles are summarized in Table 1. The total content of iron in the chemically decomposed samples was done by atomic emission spectrometry with inductively coupled plasma (SPECTRO VISION EOP, SRN). The decomposition was proceeded in a dilute $HCl+HNO_3$ (analytical grade) solution and the Fe^{II} content was subsequently determined using titration with $K_2Cr_2O_7$ solution (Czech standard CSN 722041, Part 11).

X-ray powder diffraction (XRPD) measurements were done at room temperature (RT) using D8 diffractometer by Bruker AXS equipped with a fast position sensitive detector VÅNTEC 1. The

powdered samples were pressed in a rotational holder and the patterns were carried out in a reflection mode using CoKα irradiation (λ = 0.1789 nm), Bragg-Brentano geometry, 2θ range 5 ÷ 80°, and 0.02° step.

Sample	Notation	Fe content wt. %.	FeO content wt. %.	ssa m^2g^{-1}	Mean diameter μm
anatase	A	< 0.001	< 0.001	84.9	3.88
magn. modified anatase	AM	6.47 ± 0.25	0.43±0,05	173	3.51

Tab. 1: Total content of Fe, Fe^{II} (expressed as content of FeO), specific surface area (ssa), and mean diameter of non-magnetic and magnetic anatase particles.

The morphology of particles was studied by scanning electron microscopy (SEM), PHILIPS XL-30 with spectrometer EDAX. The specific surface area of anatase particles and their size distribution were determined using laser granulometry Analysette C22.

The magnetic behavior of the magnetically modified anatase was investigated by the vibrating sample magnetometers (VSM) MicroSense EV9 and EG&G Princeton Applied Research Corporation. The room temperature magnetization (hysteresis) loop was measured up to the magnetic field ±1600 kA/m with the step of 1.6 kA/m. The thermomagnetic curve (TMC) from RT up to 924 K was obtained in an external magnetic field of 16 kA/m, temperature increase of 5 K/min and Ar atmosphere to prevent oxidation of powdered samples.

The interparticle magnetic interactions were studied using the Henkel plots $\delta M(H)$. They can be obtained from the isothermal remanence curve – $IRM(H)$ and DC demagnetization curve – $DCD(H)$ [Henkel (1964)] using the relation

$$\delta M(H) = 2\frac{IRM(H)}{IRM(\infty)} - \frac{DCD(H)}{DCD(\infty)} - 1 = 2IRM\_\mathrm{norm}(H) - DCD\_\mathrm{norm}(H) - 1, \quad (1)$$

where $IRM(\infty) \approx DCD(\infty)$ are saturation values of *IRM* and *DCD* curves. For positive values of $\delta M(H) > 0$ the interactions are connected with the exchange coupling among particles while negative values ($\delta M(H) < 0$) indicate the presence of dipolar interactions.

The nucleation behavior of TiO_2 was analyzed using the switching field distribution (SFD) that is given by the irreversible susceptibility χ_{irr}

$$\chi_{irr}(H) = \frac{d(M_{irr}(H))}{dH}, \quad M_{irr}(H) = \frac{1}{2}(1 - DCD\_\mathrm{norm}(H)). \quad (2)$$

The nucleation processes are defined as localized or delocalized instabilities of the metastable energy minimum. The peaks of the $\chi_{irr}(H)$ curve correspond with the nucleation field H_n that is defined as the magnetic field at which the nucleation occurs [Skomski et al. (1999)]. For the sake of completeness we have studied also the behavior of the reversible part of magnetic susceptibility χ_{rev} that can be described by the equations

$$\chi_{rev}(H) = \frac{d(M_{rev}(H))}{dH}, \quad M_{rev}(H) = DCD\_\mathrm{norm}(H) - \frac{hys\_pos(H)}{IRM(\infty)}, \quad (3)$$

where *hys_pos* (*H*) are the values of the hysteresis loop measured at an increasing positive magnetic field. Finally we compare the curves of the total magnetic susceptibility [Schumann (1995)] that is obtained either as a sum of χ_{irr} and χ_{rev} or from the measured hysteresis loop as d*M*/d*H*.

3 Results and discussions

The diffraction pattern of the magnetically modified anatase yields TiO_2 containing mainly the Fe_3O_4 phase as seen in Fig. 1. Nevertheless a more detailed analysis has indicated also a presence of minor maghemite (γ-Fe_2O_3) and/or hematite (α-Fe_2O_3) phases which cannot be specified more exactly due to their low content. Both TiO_2 particles, magnetically non-modified and modified, were variable in shape (Fig. 2). The iron oxide particles of diameter less than 1 μm seen by TEM (not presented here) were detected on the surface of TiO_2 particles [Safarik et al. (2013)].

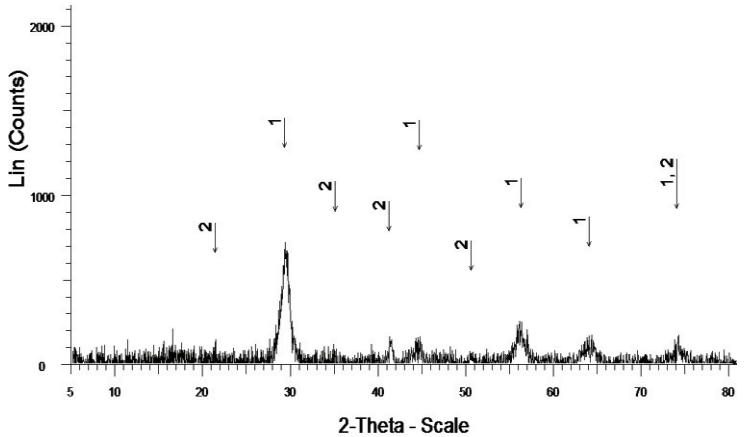

Fig. 1: The diffraction pattern of the magnetically modified TiO_2: (1) anatase; (2) Fe_3O_4 and Fe_2O_3.

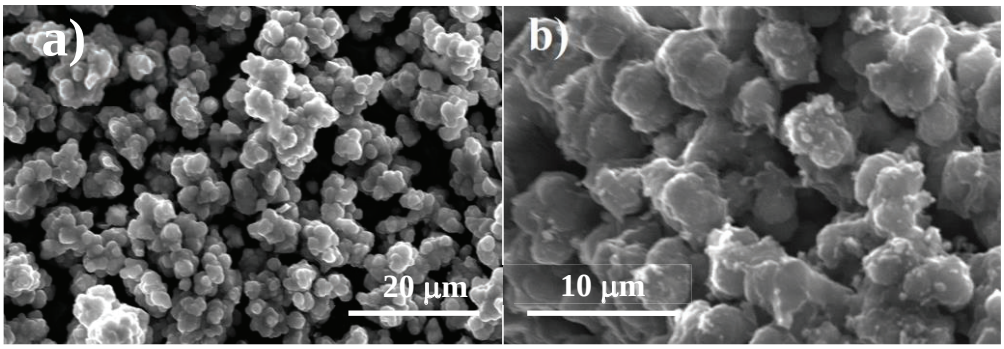

Fig. 2: The SEM image of the pure (a) and magnetically modified (b) anatase particles.

Figure 3 and Table 2 represent the hysteresis loop and the room temperature magnetic parameters of the magnetically modified TiO_2 sample. The initial coercivity and remnant magnetization (state I) are well comparable with those obtained for the phyllosilicates (montmorillonite, vermiculite, and kaolinite) magnetically modified using the same method. The marked difference in the saturation magnetization being approximately 2-3 times higher can be ascribed to the presence of magnetite yielding the highest saturation magnetization from iron oxides [Cornell et al. (1996)]. To study the

stability of core (TiO_2) and surface (shell) with iron oxide particles the thermomagnetic curve was measured. It has shown that the magnetization at the increasing temperature (Fig. 4, solid-line) reflects changes in the magnetic phase composition of the sample while the curve obtained at decreasing temperature (Fig. 4, dashed-line) documents rather the magnetic homogenizing. Because of unambiguous transformations in the iron oxides known from literature, magnetite transforms directly into hematite or through maghemite and/or ε-Fe_2O_3 [Zbořil et al. (2002), Mazo-Auluaga et al. (2003)], the observed magnetic phase transformations are induced by iron oxide modifications. A decrease around 480 K is very probably evoked by a transformation [Handea and Morrish (1977), Xu et al. (1997)] of magnetite (Fe_3O_4) into maghemite (γ-Fe2O3). The second one, around 640 K, can be ascribed to a formation of hematite [Xu et al. (1997)]. Nevertheless the magnetic transition at 850 K does not correspond with the Curie temperature of the pure hematite phase. It can be speculated about a substitution of Fe by a foreign atom, e.g. Ti, causing a decrease in temperature of the magnetic transition. Because the mutual interactions between TiO_2 and various iron oxides are not fully known, the next studies at elevated temperatures have to be done to clarify them.

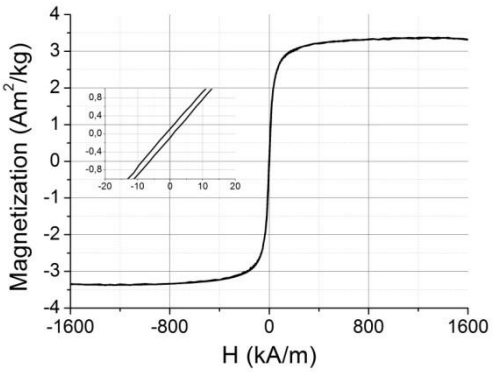

Fig. 3: RT magnetization curve of the magnetically modified anatase powder measured before the thermomagnetic treatment. The detail of the magnetization reversal is shown in the inset.

	H_c	M_s	M_r	T_c
	kA/m	Am^2/kg	Am^2/kg	K
I	1.11	3.38	0.10	820-850
II	10.77	0.74	0.14	

Table 2: Magnetic parameters obtained from the magnetization curve prior (I) and after (II) the thermomagnetic treatment (RT→924 K→RT). H_c – coercive field; M_s – saturation magnetization; M_r – remnant magnetization; T_C – Curie temperature.

The magnetization at decreasing temperature is markedly below the opposite branch and at RT it reaches values approximately 5-times lower in comparison to the initial value. This means that the temperature annealing of the magnetically modified anatase has contributed to a marked change in its magnetic phase composition. It is reflected also in the magnetic characteristics obtained at RT (Table 2, state II) evidencing more than 3 times lower saturation magnetization and approximately 10 times higher coercivity in comparison to state I. It documents an undesirable magnetic hardening of the magnetically modified sample and an instability in the magnetic phases owing to a thermal treatment connected with increasing size of the iron oxide grains.

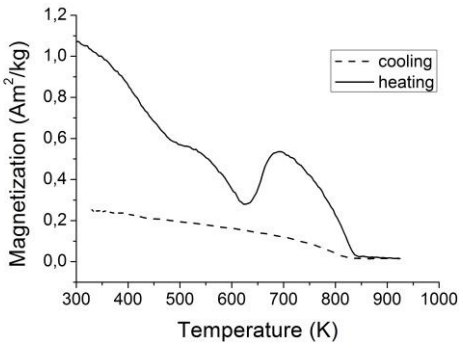

Fig 4: Thermomagnetic curve of the magnetically modified anatase. Solid and dashed lines correspond to the heating (RT → 924 K) and cooling (924 K → RT) at a constant magnetic field of 16 kA/m.

Because the iron oxide particles and their agglomerations were observed on the surface of TiO_2, the interparticle interactions will play the key role in the magnetic response of the system. From Fig. 5 it is clearly seen that the gradient of the normalized magnetization with respect to the applied magnetic field is higher in the normalized *DCD* curve (*DCD*_norm(*H*)) than in the *IRM* curve (*IRM*_norm(*H*)). This results in the prevailing negative (dipolar) interactions in the Henkel ($\delta M(H)$) plot and the condition $\delta M(H) < 0$ is fulfilled. The most important parameters, the intensity of the peak and its position on the $\delta M(H)$ curve, depend on the number of Fe atoms inside each particle. The obtained values, -0.32 and 12 kA/m, respectively, are well comparable with those determined for magnetic phyllosilicates. At higher magnetic fields (above 12 kA/m) the $\delta M(H)$ intensity decreases with increasing *H*. It becomes weakly dependent on the external magnetic field over the 80 kA/m and slowly vanishes at the field 200 kA/m.

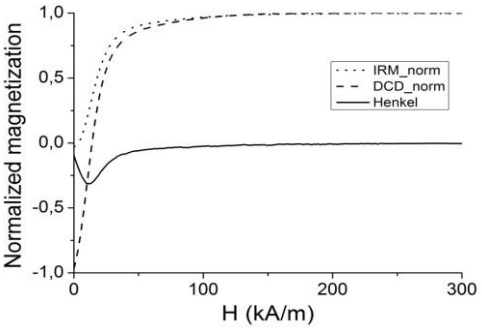

Fig. 5: Normalized isothermal remanence (*IRM*_norm) curve, normalized DC demagnetization (*DCD*_norm) curve and the Henkel plot of the magnetically modified anatase.

Generally, the magnetization of a ferromagnetic material is partly reversible and partly irreversible. The irreversible processes predetermine the main parameters of the hysteresis loop and thereby also the applicability of the investigated system. A number of factors, such as domain-wall motion, rotation of magnetization, magnetic anisotropy, etc., are responsible for the complexity of the irreversible phenomenon. The irreversible and reversible parts of the magnetic susceptibility in the magnetically modified TiO_2 analysed using relations (2) and (3) are shown in Fig. 6. The SFD curve – $\chi_{irr}(H)$ – is denoted by the dotted line and it exhibits a typical one-peak behavior. The obtained value of the nucleation field ($H_n \approx 8$ kA/m) is, however, lower than the magnetic field corresponding to the

Henkel plot peak. After reaching the peak the SFD curve gradually approximates to zero reaching it in the field of about 50 kA/m. The relatively broad SFD curve indicates a low remanence-to-saturation magnetization ratio and random orientation of iron particles. The reversible part of the magnetic susceptibility – χ_{rev} (H) – is depicted as the dot-and-dashed line and its peak-value is close to zero magnetic fields. Its approaching to zero value is in comparison with the SFD curve markedly slower. It is also reflected in the much higher value of achieved magnetic field (160 kA/m).

Both approaches chosen for calculation of the total magnetic susceptibility, (i) the sum of χ_{irr} (H) and χ_{rev} (H) depicted in the first quadrant – full line in Fig. 6, and (ii) the derivative of the magnetization curve ($\chi = dM/dH$) – dashed line, give similar but not identical results. The slight difference is caused by a presence of the low value of χ_{rev}, comparable with χ_{irr}, which documents that the reversible processes are not negligible [Schumann (1995)].

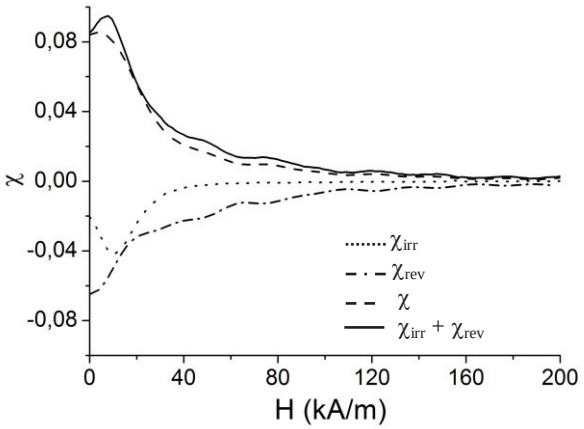

Fig. 6: Reversible (χ_{rev}) and irreversible (χ_{irr}) magnetic susceptibility established from the measured *DCD* curve. Total magnetic susceptibility expressed (i) from the magnetization curve as a dM/dH (χ) and (ii) as a sum of χ_{rev} and χ_{irr}.

4 Conclusions

A magnetically modified TiO_2 (anatase) was prepared by a simple microwave-assisted conversion of the non-magnetic precursor into its magnetic form. Submicrometer magnetic particles of dominant Fe_3O_4 with small amount of γ-Fe_2O_3 and/or α-Fe_2O_3 were deposited on the surface of anatase particles; they contributed to the relatively high saturation magnetization (3.38 Am^2/kg). A low remanence-to-saturation magnetization ratio and a broad SFD confirm random orientation of the iron oxide particles. The highest intensity of prevailing dipolar magnetic interactions and irreversible processes (nucleation field) are observed at magnetic field of 12 kA/m and 8 kA/m, respectively. The magnetic phase transformations of the iron oxides (magnetite-maghemite, maghemite-hematite) ongoing at increasing temperature during the thermomagnetic treatment resulted in the chemical and structural change of sample evoking a decrease in magnetization during cooling, a marked decrease in saturation magnetization to 0.74 Am^2/kg and a predominantly undesirable magnetic hardening of the sample at room temperature. Changes in the sample structure are then insufficient for original applications. The ferro-paramagnetic transition, the Curie temperature, of the system was detected around 850 K.

Acknowledgement

The authors thank to the financial support of the Grant Agency of the Czech Republic (Project No. 13709S/P503), the project SP 2015/168, and to the Scientific researchers of higher education institutions within the State task of the Russian Federation No. 2014/236.

References

Cornell, R.M., Schwertmann, U., 1996. in: The iron Oxides. p. 117

Fu, G., Vary, P. S., Lin, C-T, 2005. Anatase TiO_2 Nanocomposites for Antimicrobial Coatings, Journal of Physical Chemistry B 109, 8889-8898.

Handea and Morrish, 1977. Magnetite to maghemite transformation in ultrafine particles, Journal de Physique Colloques 38(C1), C1-321-C1-323.

Henkel, O., 1964. Remanenzverhalten und Wechselwirkungen in hartmagnetischen Teilchenkollektiven, Physica Status Solidi (b) 7, 919-929.

Hu, A., Apbelett, A. (Editors), 2014. Nanotechnology for Water Treatment and Purification. Springer, ISBN 978-3-319-06577-9.

Konstantinou, M, Pashalidis, I., 2008. Competitive sorption of Cu(II), Eu(III) and U(VI) ions on TiO_2 in aqueous solutions – a potentiometric study, Colloid Surface A 324, 217-221.

Mamulová Kutláková, K., Tokarský, J., Kovář, P., Vojtěšková, S., Kovářová, A., Smetana, B., Kukutschová, J., Čapková, P., Matějka, V., 2010. Preparation and characterization of photoactive composite kaolinite/TiO_2, Journal of Hazardous Materials 188, 212-220.

Mazo-Auluaga, J., Barrero, C.A., Diaz-Teran, J., Jerez, A., 2003. Thermally induced Magnetite-Hematite transformation, Hyperfine Interactions 148-149, 153-161.

Ollis, D. F., 1982. Contaminant degradation in water, Environmental Science and Technology 19, 480-484.

Safarik, I., Horska, K., Pospisikova, K., Maderova, Z., Safarikova, M., 2013. Microwave Assisted Synthesis of Magnetically Responsive Composite Materials, IEEE Transactions on Magnetics 1, 213-218.

Schumann, R., 1995. On the irreversible susceptibility of a textured Stoner-Wohlfarth ensemble, Journal of Magnetism and Magnetic Materials 150, 349-352.

Seidlerová, J., Šafaříková, M., Rozumová, L., Šafařík, I., Motyka, O, 2014. TiO_2 - Based sorbent of lead ions, Procedia Materials Science, *in press.*

Skomski, R., Liu, J.P. and Sellmyer, D.J., 1999. Quasicoherent nucleation mode in two-phase nanomagnets, Physical Review B 60, 7359-7365.

Sunada, K., Watanabe, T., Hashimoto, K., 2003. Bactericidal Activity of Copper-Deposited TiO_2 Thin Film under Weak UV Light Illumination, Environmental Science Technology 37, 4785-4789.

Svecova, L., Dossot, M., Cremel, S., Simonnot, M–O., Sardin, M., Humbert, B., Auwer den C., Michot, L., J., 2011. Sorption of selenium oxyanions on TiO_2 (rutile) studied by batch or column experiments and spectroscopic methods, Journal of Hazardous Materials 189, 764-772.

Tan, X., Wang, X., Chen, C., Sun, A., 2007. Effect of soil humic and fulvic acids, pH and ionic strength on Th(IV) sorption to TiO_2 nanoparticles, Applied Radiation and Isotopes 65, 375-381.

Trapalis, C. C., Keivanidis, P., Kordas, G., Zaharescu, M., Crisan, M., Szatvanyi, A., Gartner, M., 2003. $TiO_2(Fe^{3+})$ nanostructured thin films with antibacterial properties, Thin Solid Films 433, 186-190.

Tsydenov, D. E., Shutilov, A. A., Zenkovets, G. A., Vorontsov, A. V., 2014. Hydrous TiO_2 materials and their application for sorption of inorganic ions, Chemical Engineering Journal 251, 131-137.

Xu, W., Peacor, D. R., Dollase, W. A., Van der Voo, R., Beaubouef, R., 1997. Transformation of titanomagnetite to titanomaghemite: A slow, two-step, oxidation-ordering process in MORB, American Mineralogist 82, 1101.

Yu, J. C., Yu, J. G., Ho, W. K., Zhang, L. Z., 2001. Preparation of highly photocatalytic active nano-sized TiO_2 particles via ultrasonic irradiation, Chemical Communication 19, 1942-1943.

Zbořil, R., Mašláň, M., Barčová, K., Vůjtek, M., (2002). Thermally induced solid-state synthesis of γ-Fe_2O_3 nanoparticles and their tranformation to α- Fe_2O_3 and ε- Fe_2O_3, Hyperfine Interactions 139-140, 597-606.